FATIGUE CRACK GROWTH ACCELERATION EFFECTS UNDER HELICOPTER LOADING SPECTRA

V.Zitounis[1], P.E.Irving[1], R.Cook[2], S.Jenkins[3], D.Matthew[3]

[1] School of Industrial and Manufacturing Science, Cranfield University,
Bedfordshire, MK43 0AL, UK
[2] Deceased; Formerly, MSS, DERA, Farnborough, GU14 6TD, UK
[3] GKN-WHL, Yeovil, Somerset, BA20 2YB UK

ABSTRACT

Fatigue crack growth tests have been performed under constant and variable amplitude loading spectra on pre cracked CT specimens of titanium alloy Ti-10V-2Fe-3Al. The variable amplitude spectra were simplified versions of those previously measured on a helicopter rotorhead. They consisted of constant amplitude loading at R values of 0.7 and 0.9, interspersed with excursions to zero load or intermediate tension loads. The number of underload cycles and their frequency were systematically varied, and the resulting growth rate increment produced by 10^6 cycles of the sequence was accurately measured. The starting ΔK of the high R cycles was at the constant amplitude threshold, ΔK_{th}. It was found that crack growth rates and crack growth increments were accelerated by factors between 1.6 and 2.7 with respect to calculated linear summations of crack growth made using constant amplitude crack growth data. This is a non conservative effect. The results are discussed with respect to previous work on load interaction models.

KEYWORDS

Fatigue, crack growth, load spectra, acceleration, underloads

INTRODUCTION

Damage tolerance design philosophy, based on fatigue crack growth, is well established and applied in fixed wing aircraft. In contrast, helicopter components have been traditionally designed using safe life approaches. Damage tolerant design of helicopters requires data and understanding of how fatigue cracks develop in helicopter materials under helicopter load spectra. The application of damage tolerance analysis to helicopters presents difficulties. Marquet and Struzik [1] provide a good summary. Two problems are a) lack of understanding of fatigue crack growth in the near-threshold region and b) lack of understanding of load interaction effects under helicopter load sequences. In particular, the effect of the ground-air-ground cycles on fatigue crack growth is not well documented [2]. The load spectra of many helicopter components consists of large numbers of load cycles at high R ratio (R>0.75). The rest of the spectrum consists of load cycles at R ratios between 0.4 and 0.7, with excursions to zero load. In cracked components, stress intensity ranges (ΔK) would be close to the threshold, ΔK_{th}. Prediction of fatigue crack growth rates requires an understanding of load interaction effects under these spectra.

The behaviour of fatigue cracks under variable amplitude spectra has been studied intensively over the past 20 years. [3,4] For many load sequences, delay effects are found, compared with the growth rates predicted by a linear summation. It is well known that fatigue crack growth rates caused by small cycles following larger load excursions are slower that the linear summation damage prediction. A linear summation of crack growth is that obtained by summing the crack growth increments for constant amplitude loading, assuming no interactions between succeeding load cycles. Fatigue crack acceleration effects have been reported previously, [5] and these were found when high R ratio cycles were followed by underloads and overloads. More recently Buller et al [2] have demonstrated crack acceleration effects, compared with a linear summation, when precracked CT samples of titanium alloy Ti-10-2-3 and aluminium alloy 7010 were subjected to helicopter rotorhead spectra consisting of large numbers of near threshold cycles of R between 0.7-0.83, interspersed with excursions to zero load.

To further investigate these effects, in this study, fatigue crack growth rates were measured under two different Simple Variable Amplitude Loading (SVAL) spectra. These are simplified versions of the real helicopter rotorhead spectrum. The spectra consisted of small cycles with R ratio of 0.7-0.9, and excursions to zero load. The sequence, number and R ratio of the cycles were systematically varied. The study was conducted on Ti-10-2-3 alloy. Experimental crack growth rates were compared with those calculated using a linear summation technique, with input data from constant amplitude testing on the Ti-10-2-3 alloy.

EXPERIMENTAL PROCEDURE

Tests were performed on Ti-10-2-3 which belongs to the near beta (β) or solute-lean beta alloy class where the body centred cubic (bcc) β phase is predominant [6]. Mechanical properties of the test material are shown in Table 1.

TABLE 1
NOMINAL MECHANICAL PROPERTIES OF THE Ti-10-2-3 TEST MATERIAL

Parameter	Description	Ti-1023
σ_{UTS}	Ultimate Tensile Strength	1146 MPa
σ_{YS}	Yield Strength	1048 MPa
K_{IC}	Fracture Toughness	63.9 MPa m^1/2

Compact tension (CT) specimens (W = 70.0 mm, t = 17.5mm) were used for the research. Constant amplitude and decreasing ΔK crack growth rate data for this alloy were measured at R ratios of 0.1, 0.4, 0.7 and 0.9. In addition, fatigue tests were performed using the two load spectra shown in figure 1.

In *SVAL-1*, constant amplitude cycles at R* ratios of 0.7 and 0.9 were applied for **n** cycles, followed by **n′** cycles of underloads at R=0 (figure 1a). The starting ΔK value of the R* cycles was equal to the threshold of 1.9 MPa m$^{1/2}$ at R* of 0.7 and 1.6 for R* of 0.9. The ΔK of the R = 0 cycles was 6.3 MPa m$^{1/2}$ for R* of 0.7, and 16 MPa m$^{1/2}$ for R* of 0.9. For R* = 0.7, the number of underloads **n′** was varied from 1 to 50, keeping n constant at 1000 cycles. Additional tests were performed with **n** values between 2,000 and 50,000. A further sequence applied 1 underload every 20 small cycles with R* = 0.7. For R*=0.9, the number of test sequences was reduced to 3, with **n** of 20, 1000 and 2000; **n'** being 1, 50 and 50 respectively. All sequences were repeated for a total of 10^6 small cycles.

In *SVAL-2*, CAL at R=0.9 was applied for **k** cycles followed by CAL at R=0.7 for **k''** cycles (figure 1b). The ΔK of cycles at R=0.9 and R=0.7 was the same and was equal to the threshold value of the stress intensity factor ΔK_{th} (=1.6 MPa m$^{1/2}$) at the beginning of the test. Tests were performed such that the ratio (**k''+1**)/**k** was 0.1. The range of small cycles **k** at R=0.9 was from 100 to 10,000. This sequence was repeated for 10^6 small cycles. Unlike *SVAL-1*, this sequence contained three cycle ranges. These were **k**

cycles at R =0.9, **k''** cycles at R = 0.7, and in each individual sequence, 1 cycle of R = 0.23, this cycle being formed by the transition between the other two R ratios. This cycle had a starting ΔK of 11.6 MPa m$^{1/2}$.

Crack lengths were measured to an accuracy of ±14 μm with a high precision electrical potential system described in [7]. Tests were conducted at between 8 and 20 Hz on a digitally controlled servo hydraulic machine which controlled test loads to better than 1 % of the maximum load applied during the test. All tests were carried out in a laboratory air environment at between 15-25°C.
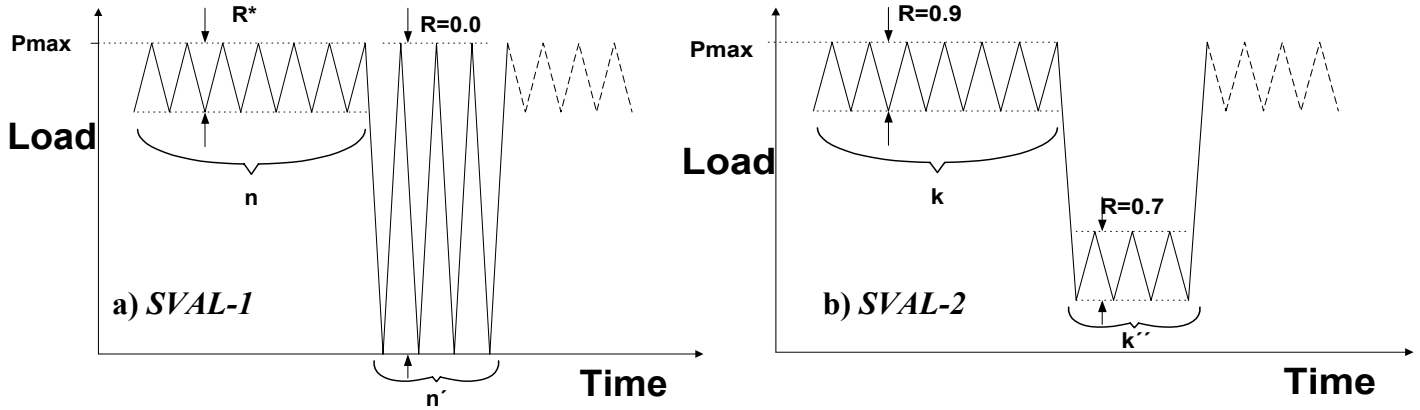

Figure 1: Definition of two different spectrums, *SVAL-1* and *SVAL-2* composed of small cycles in high R and underloads.

Crack length and cycles data were recorded automatically throughout the application of the test sequences. Crack growth rates da/dN were calculated by determining the total number of cycles of all ranges required to grow the crack successive increments of 0.1 mm. Thus the calculated da/dN was an average contribution from all types of cycle. Data were represented as crack growth increment (a) Vs total sequence cycles (N), and also as da/dN Vs ΔK. An acceleration factor γ, was defined as follows:-

$$\gamma = \frac{\text{final crack length increment measured in test } (\Delta a_{\mathrm{t}})}{\substack{\text{final crack length increment calculated by linear summation of} \\ \text{the constant amplitude crack growth data} \quad (\Delta a_{\mathrm{f}})}}$$

The linear summation calculation required crack growth integration, and was performed by the AFGROW crack growth software model [8], with no load interaction effects. The model was provided with CAL data for Ti-10-2-3, which had been measured at R = 0.1, 0.7 and 0.9. The data were curve fit, and the fitted curves used to calculate the crack growth increment produced by the completed sequences, described above. It was established that the curve fits represented the original data to an excellent accuracy in the near threshold crack growth rate regions of interest (Figure 2). The excellent agreement between experimental data for R = 0.4 and predicted line for 0.4 may be observed. The line on the extreme right of the data is that predicted for R = 0.

RESULTS

It was found that under the *SVAL-1* spectra, acceleration effects were observed only for R* values of 0.9. No acceleration effects were found under any of the *SVAL-1* spectra for R* =0.7. As the number of underloads in a sequence at R* = 0.7 increased from 1 to 50 the average da/dN increased from 10^{-11} to 10^{-10} m/cycle. However, this was a consequence of the increases in the numbers of damaging cycles and no acceleration relative to a linear summation was observed. At R* = 0.9, significant accelerations were found relative to linear summation with γ values from 1.5 to 2.2 (table 2). Fatigue crack increments Vs cycles and crack growth rates can be seen in figure 3 for these tests. ΔK in figure 3 refers to the ΔK of the small cycles in the sequence. It can be seen that the value of the ratio **n/n'**, changes the observed growth rate. For example in

figure 3b, the ratio of **n/n'** has changed to half that used for 3a, and the growth rate is reduced by about a factor of two. However the growth rate overall is accelerated relative to the linear summation by 1.5-2.2 for all sequences at R*=0.9 (Table 2).
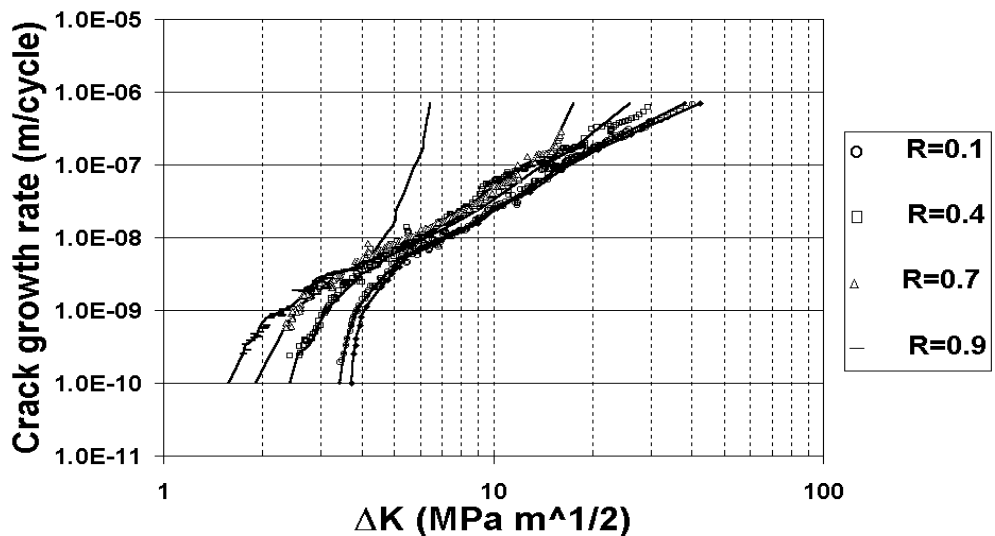

Figure 2: Fatigue crack growth rates measured experimentally (points), and curve fitted (lines)

TABLE 2
ACCELERATION FACTOR γ OBSERVED IN VARIOUS TESTS

Test condition	$n = 20$ $n' = 1$	$n = 1000$ $n' = 50$	$n = 2000$ $n' = 50$	$k = 100$ $k'' = 9$	$k = 1000$ $k'' = 99$	$k = 2000$ $k'' = 199$
Acceleration factor $\gamma = \Delta a_t / \Delta a_f$	1.66	2.19	1.52	2.55	2.67	6.32

Crack growth rates recorded for *SVAL-2* tests are presented in figure 4. Data for linear summation calculations of growth rate are also shown. The data for the test with $k = 10^4$ are not shown as the growth rate increment was too small to be accurately measured. The value of $\gamma = 6.3$ recorded with $k = 2,000$ is also subject to considerable error, as the recorded growth rate was only 10^{-10} m/cycle. The γ value calculated for each test is shown in table 2. For *SVAL-2,* there were fewer large cycles than in *SVAL-1*. Although the fraction of underloads was greater, it included the small R=0.7 cycles. γ values were 2.5-6.5 for *SVAL-2*, bigger than γ values of 1.5-2.2 calculated for *SVAL-1*. Figure 5a shows the γ factor for all tests plotted against the total growth increment obtained for each sequence. There is no clear relationship between γ and the total increment of growth obtained in 10^6 cycles. Figure 5b shows γ plotted against underload cycles expressed as a fraction of total cycles in the sequence. It shows a trend of increasing γ from 1.6 at a cycles fraction of 0.025, for *SVAL-1* to between 2.6-6 for *SVAL-2* at a cycles fraction of 0.1.

DISCUSSION

Under *SVAL-1*, only sequences with small cycles having R*=0.9 produced γ values greater than unity. No acceleration was detected for *SVAL-1* with small cycles of 0.7, despite the fact that the ΔK of the large underloads (6.3 MPa m$^{1/2}$), produced growth increments which were accurately measurable. It is concluded that acceleration effects under *SVAL-1* is confined to small cycle R ratios above R* = 0.7. Testing at R* = 0.9 produced much larger growth increments, and γ increased from 1.6 to 2.2 as the fraction of under loads increased. Testing under *SVAL-2* produced larger values of γ; despite the number of large underload cycles

being reduced. The three *SVAL-2* tests while having the same cycles ratio (0.1) differ in the frequency with which the largest cycle is applied. This appears to result in larger values of γ.
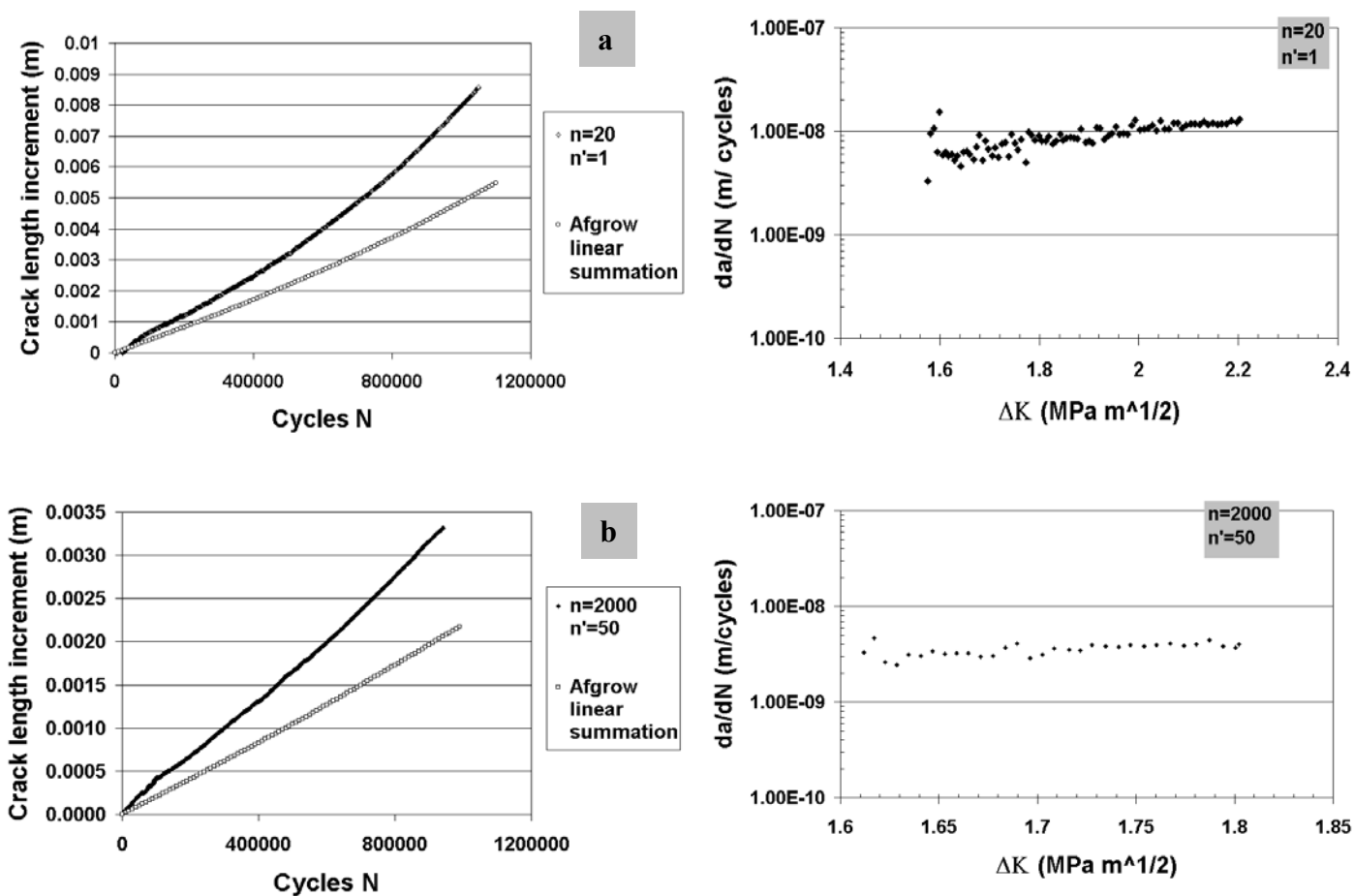

Figure 3: Comparison of measured and predicted fatigue crack growth rates under *SVAL-1* at R* = 0.9.
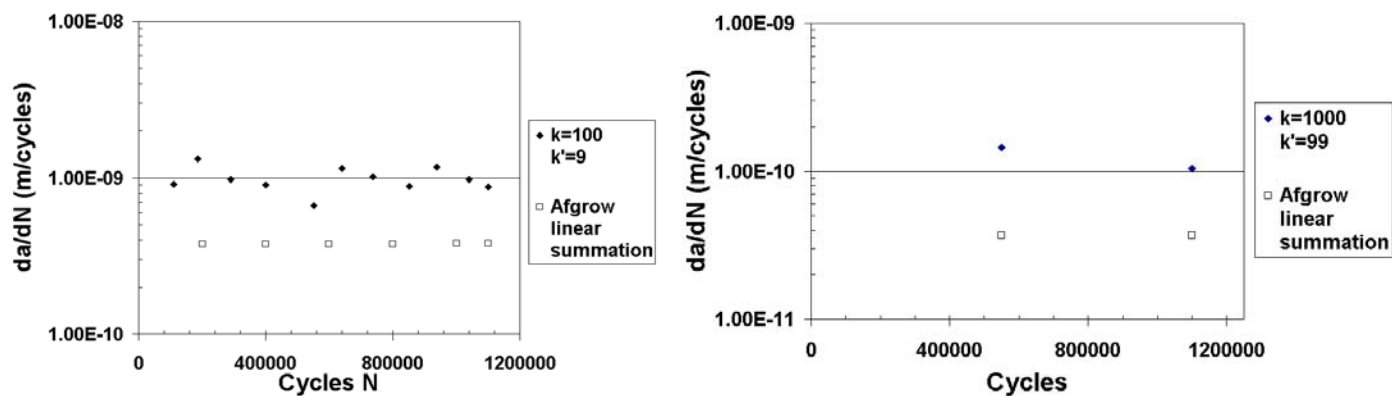

Figure 4: Comparison of measured and predicted fatigue crack growth rates under *SVAL-2* spectra.

It is unlikely that these results are a consequence of errors in constant amplitude data. Figure 2 shows excellent agreement of curve fits with the growth rate data points. In addition, the observation of changes in γ with the same cycles fraction of underloads suggests that these effects are a consequence of load interaction between low and high R cycles.

Underload effects on fatigue crack growth previously have been studied by a number of workers [5,9,10]. Acceleration effects were reported by Fleck [5], but under very different load conditions than those used in the present work. Dabeyeh & Topper [9], measured decreases in crack opening stresses as a consequence of transitions from compressive underloads to constant amplitude small cycles, up to R values of 0.8.

Accompanying transient increases in fatigue crack growth rates at R = 0.8 were found. It may be that the present results, although confined to tensile underloads, have their origin in a similar mechanism. Further work is in progress to identify the mechanism responsible and to develop adequate predictive models for fatigue crack growth under these conditions.
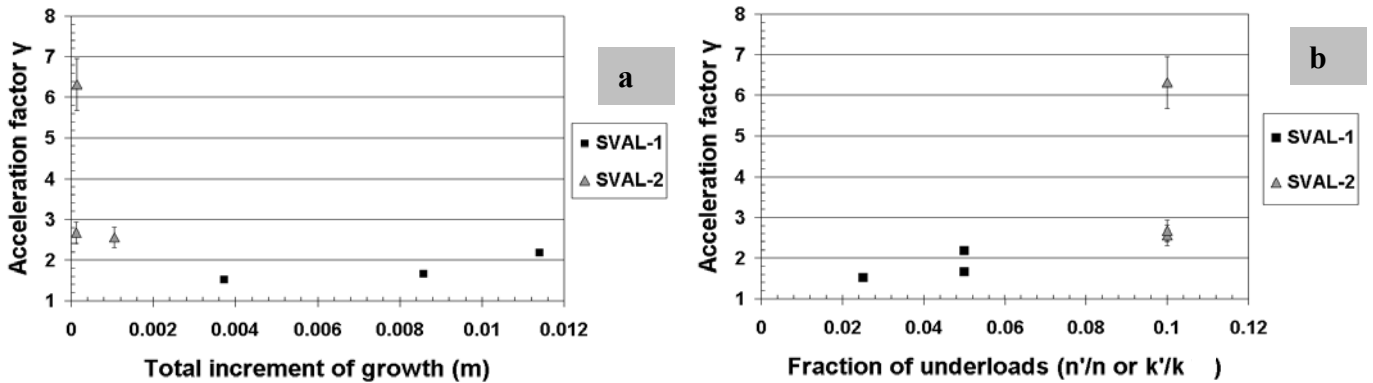

Figure 5: Variation of the acceleration factor γ with a) the total crack increment and b) Fraction of the underloads applied in each sequence of load.

Conclusions

(1) Fatigue crack growth rate testing under variable amplitude load sequences containing tensile underloads produces crack acceleration relative to a non interaction linear summation of constant amplitude crack growth rates.
(2) The acceleration relative to linear models is between 1.6 to 2.6, depending on the spectrum details.

Acknowledgements

REFERENCES

1. Marquet, T., Struzik, A., (1998). *Damage tolerance applied to metallic components*, 24th European Rotorcraft Forum, Marseilles, France.
2. Irving, P.E., Buller, R. G., (1999). In: Fatigue and Fracture Mechanics 29th vol ASTM STP 1332, pp 727-742, Panontin, T.L., Sheppard. S.D. (Eds). American Society of Testing and Materials, USA
3. Kumai, S., Higo, Y. (1996). *Materials Science and Engineering A221*, 154
4 Sadananda, K., Vasudevan, A. K., Holtz, R. L., Lee, E. U, (1999). *Int. J. Fatigue 21*, 23
5. Fleck, N. A., (1985). *Acta Metall. Vol33, No 7,* 1339
6 Buller, R.G., Jenkins, S., (1998). Final report *WP320-Material Data and component tests on WHMS 640 (Ti-10V-2Fe–3Al)*, GKN Westland Helicopters, LR97,182 DTI-LINK RA/6/30/06
7. Wei, R. P., Brazil, R. L., (1981). In: *Fatigue Crack Growth Measurement and Data* Analysis ASTM STP 738, pp. 103-119, S.J. Hudak, Jr. and R. J. Bucci (Eds), American Society of Testing and Material, USA
8. Harter, James A., (2000) *AFGROW Users manual, Version 4.0001.11.8, Technical Memorandum,* AFRL-VA-WP-TR-2000-XXXX, AFWAL Flight Dynamics Laboratory, Wright-Patterson AFB, OH.
9. Dabayeh, A.A., Topper, T.H., (1995). *Int. J. Fatigue* 17, 261
10. Hackyard, M., Powell, B.E., Stephenson, J.M., McEIhome, M., (1999). *Int. J. Fatigue* 21, S59